# One-pot synthesis of chitosan/iron oxide nanocomposite as an eco-friendly bioadsorbent for water remediation of methylene blue

*Mina Keshvardoostchokami*[1,2], *Farideh Piri*[1], *Abbasali Zamani*[2] ✉

[1]*Organic Chemistry Research Laboratory, Department of Chemistry, Faculty of Science, University of Zanjan, Zanjan 45371-38791, Iran*
[2]*Environmental Science Research Laboratory, Department of Environmental Science, Faculty of Science, University of Zanjan, Zanjan 45371-38791, Iran*
✉ *E-mail: zamani@znu.ac.ir*

Published in Micro & Nano Letters; Received on 12th November 2016; Revised on 17th January 2017; Accepted on 19th January 2017

Chitosan/iron oxide nanocomposite was synthesised via a one-pot method, then its functional groups and morphological structure were characterised by Fourier transform infrared spectroscopy, field emission scanning electron microscopy, transmission electron microscopy, Brunner, Emmett, and Teller analysis and energy-dispersive X-ray spectroscopy. The synthesised nanoparticles had an average particle size of 50 nm with a surface area, total pore volume and mean pore diameter of the nanocomposites calculated at 0.46 $m^2/g$, 0.11 $cm^3/g$ and 53.209 nm, respectively. After characterisations, the nanoparticles were applied as the bioadsorbent for aqueous solutions, which were polluted with methylene blue as a model of cationic dyes. The maximum adsorption capacity obtained was 5.12 mg/g. The study parameters influencing the adsorption processes show that 0.2 g of chitosan/iron oxide nanocomposite removed 80% of the pollution (initial concentration 10 mg/l) from 50 ml of water with a pH > 4 after 60 min at 25°C, while unmodified chitosan removed only 20%. The nanoparticles were able to remove over 50% of the dye after five reused cycles. The application of different salts revealed that sodium chloride had a greater restraint effect than sodium sulphate on the adsorbent. The pseudo-second-order and the Langmuir model successfully exhibited the adsorption kinetic and isotherm.

**1. Introduction:** Chitosan as a natural polymer was produced from an abundant biopolymer called chitin. The existence of active functional groups on its surface converts it to a highly efficient adsorbent [1]. On the one hand, biopolymer nanocomposites have significant interest due to their environmentally friendly, nontoxicity, biodegradability and low-cost characteristics [2]; on the other hand, the profitable characterisations of chitosan, especially dissolution in different media, improved its adsorption ability and its application for water sanitation [3, 4]. These arguments incite authors to synthesise chitosan nanocomposite as an eco-friendly adsorbent.

Different composites of chitosan with various goals were synthesised; for example, a synthesised chitosan/silver nanocomposite with different amounts of silver was used as a colorimetric sensor [5]. Also, a hybrid nanocomposite of chitosan and graphene was synthesised, which can be used to fabricate a dopamine selective electrode [6]. Chitosan/starch nanoparticles were utilised as carriers in the drug delivery of bis-desmethoxycurcumin [7]. Therefore, water sanitation is another important usage of chitosan nanocomposites [8].

The cleaning of the environment compartments from dyes pollutions is unavoidable because of their abundant use on one hand, and their complex aromatic structures on the other hand, which cause allergic dermatitis, cancer and mutations [9, 10]. Some dyes are added to food products in the form of food additives in order to improve the external appearance of the natural products; as a result, these can pose a threat to human health [11]. Orange II, a type of azo-dye, is applied in many industries and which causes blood diseases [12]. Dyes could also affect the food chain by adsorption and reflection of sunlight. The different physical, chemical and biological methods are applied for treatment of aqueous solutions polluted with dyes [8, 13–15]. Most of these methods are expensive and time consuming and are, therefore, rarely used. Due to special characteristics such as low cost and applicability of some natural adsorbents in water treatment, natural adsorbent is also notable for this purpose [16–18]. A novel adsorbent, namely magnetic $Fe_2O_3$/chitosan composite, was fabricated by a micro-emulsion process and its application investigated for the removal of azo-dyes [19]. A γ-$Fe_2O_3$/$SiO_2$/chitosan composite is another chitosan composite that is synthesised by water-in-oil emulsification and used in the sanitation of water solutions polluted with methyl orange [20].

Methylene blue (MB), a cationic dye, is commonly used in textile manufacturing as a colorific agent for different tissues [21]. Several researchers are calling for the removal of MB due to its harmful impact on health [22–28]. Batch and fixed-bed adsorption methods have been used for confirming the ability of new synthesised adsorbents. A batch adsorption experiment is a common method in academic research with the aim of funding profitable and economical adsorbents [29–31]. Furthermore, these studies also provide information about the design of water treatment systems that are used on an industrial scale.

In this Letter, after the fabrication and characterisation of inexpensive (in comparison with carbon nanotubes and grapheme compounds) and environmentally friendly chitosan/iron oxide nanocomposite, (CH–FeO nanocomposite), the abilities and properties of the adsorbent are evaluated for removal of MB as a model for cationic dyes from polluted water solutions. Besides the effect of different parameters on the removal procedure, the reusability and inorganic salt on MB adsorption was investigated and discussed. Also, kinetics and isotherm parameters were evaluated. This Letter introduces a modified method in synthesised CH–FeO nanocomposites, which is a low-cost and easy method. The synthesised CH–FeO nanocomposite is used for the removal of pollutants that enter the food chain, thus causing a serious threat to health. Also, this is a new application of CH–FeO nanocomposite as a cationic dye eco-friendly biosorbent.

## 2. Experimental section

2.1. Chemicals: MB (115943, Merck), sodium chloride (106406, Merck), disodium sulphate (106649, Merck), acetic acid (100063, Merck), ferric chloride (803945, Merck), hydrochloric acid




doi: 10.1049/mnl.2016.0681

**Table 1** Effect of different ratios of CH–FeO nanocomposite ($FeCl_3$/chitosan) on removal of MB

| $FeCl_3$/chitosan | 0.1/0.4 | 0.15/0.4 | 0.2/0.4 | 0.3/0.4 | 0.35/0.4 | 0.4/0.4 |
|---|---|---|---|---|---|---|
| %MB removal | 20.89 | 35.00 | 49.02 | 52.45 | 45.00 | 27.49 |

(100317, Merck) and sodium hydroxide (106498, Merck) with analytical grade were purchased and used as chemicals in synthesise of composite and in the removal study step. Medium molecular weight chitosan with a de-acetylation degree of 75–85% was purchased from Sigma-Aldrich Chemical. All chemicals were used without further purification.

2.2. Synthesise of CH–FeO nanocomposite: To synthesise CH–FeO nanocomposite as an adsorbent, in step one 0.4 g of chitosan was dissolved in 50 ml of acetic acid solution (1% v/v), then 0.3 g of $FeCl_3$ was added in an ultrasonic bath (Bandelin DT102H). In step two, 20 ml NaOH solution 8 M was added and sonication was continued for 10 min. The precipitants as product were laundered several times with distilled water and then the mixture was centrifuged (Universal 320 bench-top centrifuge) at a speed of 2000 rpm. The product was then air-dried. The applied method was designed with modification reported method by Lv *et al.* in 2014 [32].

2.3. CH–FeO adsorbent characterisation: For the study of surface characterisation and determination of particle size, field emission scanning electron microscopy (FE-SEM) and transmission electron microscopy (TEM) were used. In this Letter, field emission scanning electron microscope Mira 3-XMU model and TEM Zeiss EM900 model were applied. Fourier transform infrared (FTIR) spectra of the synthesised nanocomposites were recorded with a Nicolet iS10 FTIR spectrometer in the wavelength range of 4000–400 $cm^{-1}$, in the attenuated total reflection mode. A surface area analyser (Belsorp, BELMAX, Japan) was applied in the assessment of the specific surface area of the synthesised CH–FeO nanocomposite.

2.4. Kinetic and equilibrium adsorption studies in batch experiment: The mixture of 50 ml MB with initial concentration (10 mg/l) and 0.2 g of CH–FeO nanocomposite was put in an Erlenmeyer flask. The mixture was stirred on a shaker (IKA KS 260) at a speed of 300 rpm for 60 min at 25 ± 2°C. To set the pH of the solution, diluted HCl or NaOH (0.01 M) was used. Phase separation was performed by centrifuge (Universal 320) at 2000 rpm. An analysis of the dye was carried out using a UV–Vis spectrophotometer (Analytikjena 205). The maximum wavelength for MB is 668 nanometer ($\lambda_{max} = 668$). For the calculation of the amount of adsorption capacity in equilibrium time, and dye adsorbed ($q_e$, mg/g), (1) was used

$$q_e = \frac{(C_0 - C_e)V}{M_s} \quad (1)$$

where '$C_0$' and '$C_e$' (mg/l) are initial and equilibrium concentrations of the MB solution, respectively; '$V$' (l) is the volume of the dye solution and '$M_s$' in the equation means mass (g) of the utilised nanocomposite. All results are means of experiments performed in triplicate. From four different ratios of the synthesised composite in identical conditions, the ratio of 0.3 g of $FeCl_3$ to 0.4 g of chitosan showed the best removal result for MB. We therefore continued the elimination tests by this ratio of the synthesised composite (Table 1).

2.5. Fixed-bed adsorption experiment: To determine the potency of CH–FeO nanocomposite as fillers in a fixed-bed column, the experiments were carried out by using a 2 ml syringe, which was filled with 0.08 and 0.16 g of the CH–FeO adsorbent corresponding to 0.1 and 0.2 ml bed heights. 50 ml MB solution (with concentration 10 mg/l) was passed drop by drop. After passing all 50 ml of the dye solution from the column, the MB concentration was measured in the passed solution.

2.6. Regeneration of adsorbent: For the regeneration test, the dried used adsorbent was agitated in 200 ml acidified distilled water (pH 4 by using HCl 0.1 M); this procedure was repeated twice. Then, the adsorbent was stirred in 300 ml distilled water and adjusted to pH 12 by 0.1 M NaOH. This cycle was repeated three times [3].

2.7. pH at the point of zero charge ($pH_{pzc}$): The pH that the total number of positive and negative charges on the adsorbent surface are equal was named as the point of zero charge ($pH_{pzc}$) [33]. This pH is a term relating to the phenomenon of adsorption and is used to describe the pH dependency. The pH drift method was used in the determination of the $pH_{pzc}$ of CH–FeO nanocomposite. The pH of 50 ml of NaCl solutions (0.005 mol/l) was set between 2 and 12 by adding diluted HCl or NaOH. About 0.08 g of adsorbent was added in NaCl solutions and shaken for 24 h at 25 ± 2°C. The graph of the final and initial pH was drawn and used for the identification of $pH_{pzc}$ [34].

## 3. Results and discussion

3.1. Characterisation of synthesised CH–FeO nanocomposites: One method for the characterisation of nanocomposites is the FTIR spectra, of which the following peaks for chitosan were reported: 3456 $cm^{-1}$ for O–H stretching bond and N–H stretching bond, 1657 $cm^{-1}$ for C=O of –NH=C=O bond stretching (amide I), 1600 $cm^{-1}$ for N–H blending modes (amide II), 1423 $cm^{-1}$ ascribes to –C–O stretching of primary alcoholic group on the surface of adsorbent, 1077 and 1030 $cm^{-1}$ for C–OH stretching bond [35]. Most studies have reported that magnetic chitosan shows a peak in ∼580 $cm^{-1}$ (Fig. 1*a*) for the Fe–O group due to pure $Fe_2O_3$ [36]. As shown in Fig. 1*a*, the shifting of O–H and N–H bonds from 3456 to 3445, C=O of –NH=C=O stretching bond (amide I) from 1657 to 1606 and N–H blending modes (amide II) from 1600 to 1592 indicates that Fe and chitosan were combined successfully. The same data was reported by Lv *et al.*, in synthesis of cross-linked Fe(III)-chitosan complex [32].

Before and after adsorption of the pollutant, spectra were compared. For peaks at 1606 and 1592 which could be attributed to C=O of –NH=C=O stretching bond (amide I) and N–H blending modes (amide II) were moved to 1635 and 1630 after adsorption (Fig. 1*a*). This shifting means that, by adsorption of MB on the surface of the composite, Fe will be involved in the dye molecule which causes a weak interaction with the chitosan functional groups.

In Fig. 1*b*, FE-SEM and TEM images of fabricated nanocomposite are shown to study the particle size and morphology. The average particle sizes are under 50 nm. Porous morphology of CH–FeO nanobiocomposite reveals the incorporation of iron oxide nanoparticles in CH, indicating the formation of CH–FeO hybrid nanobiocomposite.

The energy-dispersive X-ray (EDS) spectra of CH–FeO nanocomposite confirmed the peak of C, O, N and Fe, as the four major atoms of the composite and the existence of chitosan and $Fe_2O_3$. The results from EDS indicate that 6% of the synthesised nanocomposite is assigned to Fe nanoparticles. The surface area of the synthesised nanocomposites was determined by nitrogen adsorption. The Brunauer–Emmett–Teller analysis verified that the surface area, the total pore volume and mean pore diameter of synthesised nanocomposites are 0.46 $m^2/g$, 0.11 $cm^3/g$ and 53.209 nm, respectively.

3.2. Adsorption procedure of MB with synthesised CH–FeO nanocomposite: Fig. 2 shows the consequences for the uptake of

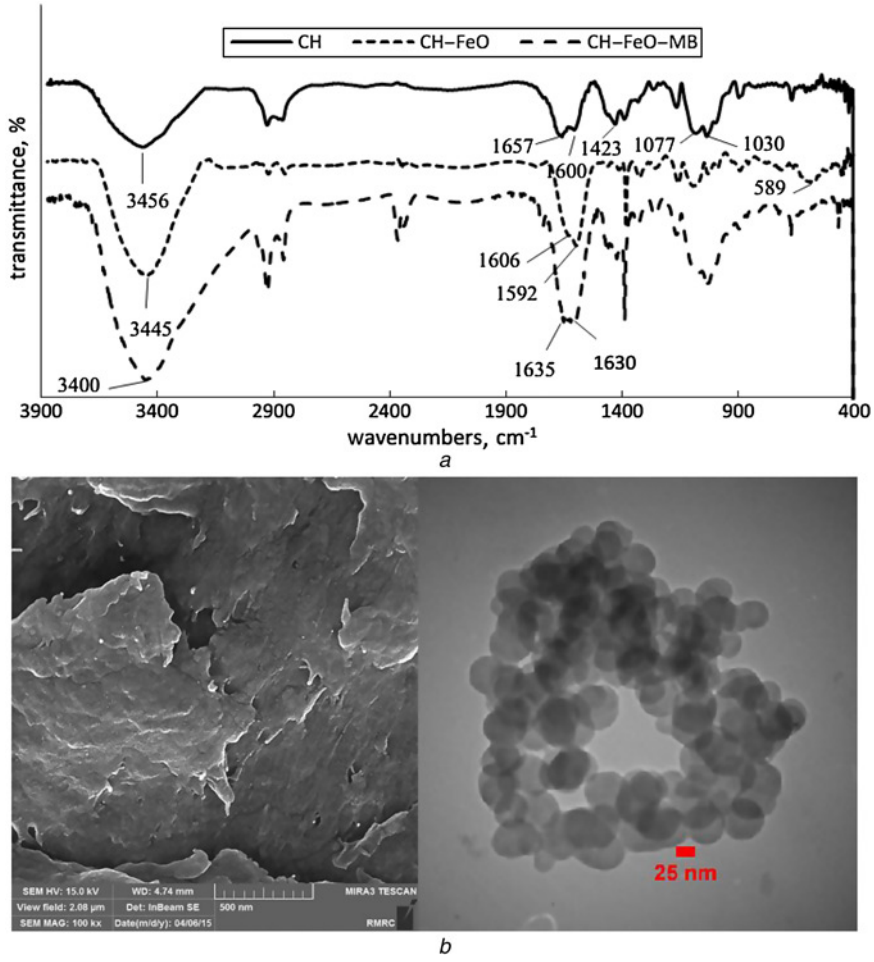


**Fig. 1** *FTIR-spectra, FE-SEM and TEM images*
*a* FTIR-spectra of CH, CH–FeO and CH–FeO-MB
*b* FE-SEM and TEM images of CH–FeO nanocomposite

MB at different contact times where other experimental conditions are constant. Results confirm increasing adsorption when contact time was raised. The maximum adsorption was seen after 10 min. It can be a vindicating for the formation of a monolayer of adsorbed ions on the surface of the nanocomposite. This can be explained by numerous active sites on CH–FeO, which outstripped the scanty molecules of adsorbates in low concentrations and contest for limited actives for numerous adsorbate molecules at higher concentrations [3]. Increasing the initial concentration increases the number of interactions between the dye and adsorbent functional groups on the surface of the adsorbent [3].

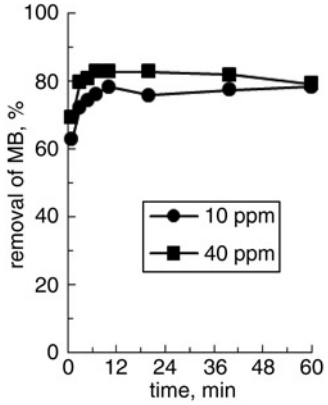


**Fig. 2** *Time dependency and effect of initial concentration of MB on the adsorption procedure with CH–FeO nanocomposite. Experimental conditions: volume of dye 450 ml, pH 6.5, weight of adsorbent 0.72 g, shaking rate 300 rpm, temperature 25°C*

3.3. Kinetics of MB adsorption with synthesised CH–FeO nanocomposite: To study the mechanism of adsorption and potential rate of the controlling steps, such as mass transport and chemical reaction processes, kinetic models have been used to test experimental data. Power function (2), simple Elovich (3), pseudo-first-order (4) and pseudo-second-order kinetics (5) are useful models in the adsorption kinetics study [36]. Equations (2)–(5) illustrate the used models

$$\log q_t = \log k_{\mathrm{p}} + \nu \log t \tag{2}$$

$$q_t = a + 2.303 b \log t \tag{3}$$

$$\log (q_{\mathrm{e}} - q_t) = \log q_{\mathrm{e}} - \frac{k_1 t}{2.303} \tag{4}$$

$$\frac{t}{q_t} = \frac{1}{k_2 q_{\mathrm{e}}^2} + \frac{t}{q_{\mathrm{e}}} \tag{5}$$

In these equations, '$t$' in (2) is the contact time (min) and '$q_t$' is the amount of adsorbed dyes on the surface of the adsorbent (mg/g) at time '$t$'. '$k_{\mathrm{p}}$' (mg/g min) and '$\nu$' are setting parameters for the power function model. In a simple Elovich model (3), the parameter '$a$'




doi: 10.1049/mnl.2016.0681

**Table 2** Kinetic model parameters for MB adsorption on the synthesised CH–FeO nanocomposite

| Pseudo-first order | | Power function equation | | | Simple Elovich | | | Pseudo-second order | | |
|---|---|---|---|---|---|---|---|---|---|---|
| $k_1$ | $R^2$ | $R_2$ | $v$ | $k_p$ | $a$ | $b$ | $R^2$ | $k_2$ | $q_e$ | $R^2$ |
| −0.03 | 0.456 | 0.69 | 0.044 | 4.21 | 4.216 | 0.197 | 0.704 | 0.741 | 4.897 | 0.999 |

(mg/g min) demonstrates the rate of chemisorption, and the parameter '$b$' (g/mg) is the desorption constant. These parameters are related to the extent of surface coverage and the activation energy for the adsorption. In (4), '$q_e$' is the amount of adsorbed MB on the surface of the used nanocomposite as the adsorbent (mg/g) at equilibrium condition. Also in this equation, '$k_1$' denotes the pseudo-first-order rate constant (1/min). In (5), '$k_2$' indicates the rate constant for this model in g/mg min.

Equation (6) was used as a calculation of the initial rate of sorption

$$h_0 = k_2 q_{2e} \tag{6}$$

In this equation, '$h_0$' denotes the initial rate of sorption (mg/g min).

The kinetic parameters assessed were based on the used kinetics models for the uptake of MB on CH–FeO nanocomposite (Table 1). The given constants and regression coefficient ($R^2$) of the studied models show that three power function, simple Elovich and pseudo-first-order kinetic models, do not appropriately exhibit the experimental adsorption results. However, the pseudo-second-order kinetic models, as with other researches, have high collation and a significant correlation with the description of MB adsorption on the surface of the used nanocomposite in this procedure. Kinetic calculated parameter models, '$K_2$' and '$R_2$', were 0.741 and 0.999, respectively. The initial rate of adsorption is 17.77 mg/g min. This processes the same as other studies obeyed pseudo-second-order kinetics [4, 23, 24]. There is a good correlation between the amounts of calculated $q_e$ from the pseudo-second-order model and the given amounts from the experimental study 4.897 (Table 2), 5.12 (Table 3), respectively.

3.4. pH dependence of MB uptake with synthesised CH–FeO nanocomposite: The investigation of pH is important in the adsorption processes because of the changes in protonation and deprotonation of the synthesised nanocomposite functional groups and, as a result, its efficiency on the uptake of MB as a cationic dye. Although chitosan naturally has a positive surface because of the protonation of $–NH_2$ groups, during synthesis of the composite by the addition of NaOH, $–NH_3^+$ groups convert to $–NH_2$ groups which cause better adsorbent for cationic remediation. The experiments were planned to peruse the effect of this parameter on the removal efficiency. About 0.08 g of synthesised CH–FeO nanocomposite was added to 50 ml of aqueous solution containing 10 mg/l of MB and adjusted to pH of 1–9. After 60 min of shaking, the mixture was filtered and the amount of dye remaining in the aqueous phase was determined spectrophotometrically. Fig. 3*a* shows that adsorption efficiency increased as the pH of the solutions increased. The charges of adsorbent and sorbent are the same at a lower pH of the solution. This can cause a repulsion of MB molecules of CH–FeO nanocomposite surface [37]. However, by increasing the pH of the solution, $–NH_3^+$ and FeOH groups transfer to $–NH_2$ and $–FeO^-$ groups, which cause surface strenuous sites between CH–FeO and the cationic MB molecules. On the other hand, at basic media there is electrostatic attraction between $–COO^-$ groups and MB molecules [3]. The suggested mechanism is represented in Fig. 4.

**Table 3** Characterisation of the studied adsorbent and other different adsorbent for adsorption of MB

| Adsorbent | $q_e$, mg/g | Kinetic model | Isotherm model | Reference |
|---|---|---|---|---|
| MBC–CH | 142 | pseudo-first order | Redlich–Peterson | [3] |
| MGO | 64.23 | pseudo-second order | Langmuir | [27] |
| CCSB | 95.24 | pseudo-second order | Langmuir | [4] |
| Canola | 16.7 | pseudo-second order | Sips | [28] |
| PProDOT/$MnO_2$ | 12 | pseudo-second order | Langmuir | [38] |
| PP-GP | 4.24 | pseudo-second order | chemisorption | [39] |
| NZVI/SuZSM | 86.7 | pseudo-second order | Langmuir and Freundlich | [40] |
| CH–FeO | 5.12 | pseudo-second order | Langmuir | this work |

Modified ball clay/chitosan composite (MBC–CH), magnetic graphene oxide (MGO), crosslinked chitosan/ bentonite composite (CCSB), Canola residues, chitosan/iron oxide nanocomposite (CH–FeO), poly (3,4-propylenedioxythiophene)/$MnO_2$ composites (PProDOT/$MnO_2$), pyrophyllite pickling–grinding powders (PP-GP), modified zeolite adsorbent containing nanoscale zero-valent iron (NZVI/SuZSM).

3.5. Finding of point of zero charge ($pH_{pzc}$) of CH–FeO nanocomposite: A study of point of zero charge of CH–FeO nanocomposite and values of the final and initial pH of the electrolyte and adsorbent solution (Fig. 3*b*) show that the surface

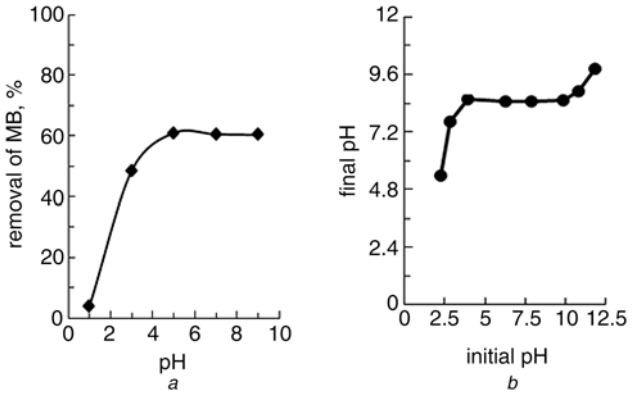


**Fig. 3** *Effect of aqueous solution pH on MB uptake by the CH–FeO nanocomposite as adsorbents*
*a* Effect of aqueous solution pH on MB uptake by the CH–FeO nanocomposite as adsorbents. Experimental conditions: volume of dye 50 ml, weight of adsorbent 0.08 g, shaking rate 300 rpm, shaking time 60 min, temperature 25°C
*b* Point of zero charge of synthesised CH–FeO nanocomposite

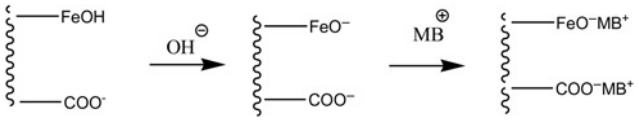


**Fig. 4** *Proposed changing the surface of CH–FeO nanocomposite with aqueous solution pH*

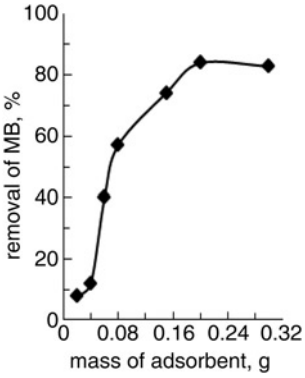


**Fig. 5** *Effect of CH–FeO nanocomposite dose on MB uptake in adsorption procedure. Experimental conditions: volume of dye 50 ml, pH 6.5, shaking rate 300 rpm, shaking time 60 min, temperature 25°C*

of the CH–FeO composite has a positive charge before pH 4. In the pH range 4–10, the more surface has zero charge. The results confirm that after higher pH than 10 charge of surface change to negative. So, the best pH for the removal of cationic dyes is higher than 4.

3.6. Adsorption dependency to amount of synthesised CH–FeO nanocomposite: The uptake of MB adsorption effects was studied as a function of adsorbent amount (0.02–0.3 g). The solution pH was fixed to 6.5 ± 0.2 and the initial concentrations of MB used were 10 mg/l. The results showed that increasing the quantity of adsorbent increased the uptake efficiency (Fig. 5). It was found that the quantity of 0.2 g of CH–FeO *nanocomposite* cans quantitatively uptake MB as a dye pollutant from 50 ml contaminated dye solution.

3.7. Effect of inorganic salt on MB adsorption with synthesised CH–FeO nanocomposite: The effect of type and amount of electrolyte on the uptake of MB on the surface of CH–FeO nanocomposite was investigated by the addition of NaCl and $Na_2SO_4$ salts. The solution matrix and presence of salts can alter the efficiency of the adsorption process. For this purpose, MB removal from four aqueous phases containing ~0.5 and 1 M salts of NaCl and $Na_2SO_4$ was verified. These salts are in abundance in most real and industrial waters and waste waters. The decrease in the uptake of MB is probably the result of adsorption competition between the cations of the salts and MB dye. A variation in the activity coefficients by salt concentration must also be considered [3].

3.8. Regeneration of CH–FeO nanocomposite as adsorbent: The regeneration study was tested in order to reuse CH–FeO nanocomposite as adsorbent. After five reused cycles, the synthesised nanoparticles uptake was above 50% of MB from polluted solution. The reason for high adsorption for CH–FeO composite after regeneration cycles can be attributed to repulsion interaction between the MB molecules and the protonated surface of CH–FeO nanocomposite in acidic media and activation of the nanocomposite surface by agitation in basic solution.

3.9. Adsorption isotherms: In this research of adsorption isotherms, the most widely used models of Langmuir, Freundlich, Temkin and Dubinin-Radushkevich were used, the data of which are shown in Table 3. Adsorbent uptake on a homogenous surface, monolayer adsorption and non-existence interaction between the surface and adsorbent are hypotheses of the Langmuir model in the adsorption procedure. The Freundlich model assumes that the adsorption of adsorbent occurs on a heterogeneous surface by multilayer adsorption. The Temkin isotherm claims that the decrease in the heat of adsorption is linear rather than logarithmic, as in the Freundlich model. In the Temkin model, the adsorption heat of all adsorbent molecules in the adsorbed layer should decrease linearly with coverage from the adsorbed/adsorbent interaction. The hypothesis of Dubinin-Radushkevich isotherm is similar to the Freundlich model [41, 42].

For the study of the Langmuir isotherms, we must draw the adsorption equilibrium capacity against the concentration of adsorbent in the aqueous solution. Equations (7) and (8) are exponential and linear and simple forms of Langmuir isotherms

$$q_e = \frac{bQ_{max}C_e}{1 + bC_e} \tag{7}$$

$$\frac{C_e}{q_e} = \frac{1}{q_{max}b} + \frac{C_e}{q_{max}} \tag{8}$$

where '$C_e$' denotes the concentration of MB in aqueous solution at equilibrium conditions with scale mg/l; '$q_e$' means the amount of dye adsorbed in mg by 1 g of adsorbent at equilibrium time (mg/g); '$q_{max}$' is the maximum adsorption capacity of the adsorbent; and '$b$' is the constant for the binding energy of the adsorption system.

In this Letter, the Langmuir adsorption isotherm constants ($b$ = 0.73, $q_{max}$ = 1.52) and correlation coefficients ($R^2$ = 0.89) show that the data was reasonably well fitted to this model than others, indicating homogenous surface binding.

3.10. Application of CH–FeO nanocomposite in fixed-bed adsorption: The fixed-bed column method for the removal of MB dye was investigated in batch-optimised conditions. The composite removed 55 and 62% when the column was filled with 0.08 and 0.16 g of adsorbent.

**4. Conclusion:** In this Letter, the authors have reported a new and environmentally friendly adsorbent in water treatment which is fabricated by way of a simple procedure. Also, this Letter confirms the synthesis of CH–FeO nanocomposite and its potential for the sanitation of aqueous solutions polluted with MB in the batch method. Under optimised effective parameters in the procedure, including contact time of 60 min and 0.2 g of synthesised CH–FeO nanocomposite as adsorbent dose for 50 ml of aqueous solution with pH 8 and initial MB concentration 10 mg/l, the amount of the MB uptake was 80% at 25°C, while for the fixed-bed column the MB adsorbed about 65%. It was found that the used nanocomposite adsorbent is usable after five regeneration cycles. Furthermore, it should be considered that the adsorbent can be collected from water because of iron oxide magnetic potential. Our synthetic composite from the point of view of adsorption capacity is lower when compared with adsorbents, such as modified ball clay/chitosan composite, magnetic graphene oxide, cross-linked chitosan/bentonite composite, Canola residues, poly(3,4-propylenedioxythiophene)/$MnO_2$ composites and pyrophyllite pickling-grinding powders, but the synthesised adsorbent regenerates and can be reused easily five times (Table 3). The agreement between the adsorption capacity of adsorbent obtained by the kinetic model and the experimental method shows that the uptake mechanism is well established. This information may be useful for the removal of the other dyes from this class.

**5. Acknowledgments:** The authors thank especially the students and members of the Environmental Science Research and Dr Taghipour Laboratories, University of Zanjan, Zanjan-Iran, for their contributions to this research.

## 6 References

[1] Johns J., Rao V.: 'Adsorption of methylene blue onto natural rubber/chitosan blends', *Int. J. Polym. Mater.*, 2011, **60**, pp. 766–775




doi: 10.1049/mnl.2016.0681

[2] Sadeghi-Kiakhani M., Arami M., Gharanjig K.: 'Preparation of chitosan-ethyl acrylate as a biopolymer adsorbent for basic dyes removal from colored solutions', *J. Environ. Chem. Eng.*, 2013, **1**, pp. 406–415
[3] Auta M., Hameed B.: 'Chitosan–clay composite as highly effective and low-cost adsorbent for batch and fixed-bed adsorption of methylene blue', *Chem. Eng. J.*, 2014, **237**, pp. 352–361
[4] Bulut Y., Karaer H.: 'Adsorption of methylene blue from aqueous solution by crosslinked chitosan/bentonite composite', *J. Dispersion Sci. Technol.*, 2015, **36**, pp. 61–67
[5] Nivethaa E., Narayanan V., Stephen A.: 'Synthesis and spectral characterization of silver embedded chitosan matrix nanocomposite for the selective colorimetric sensing of toxic mercury', *Spectrochim. Acta A, Mol. Biomol. Spectrosc.*, 2015, **143**, pp. 242–250
[6] Liu C., Zhang J., Yifeng E., *ET AL.*: 'One-pot synthesis of graphene–chitosan nanocomposite modified carbon paste electrode for selective determination of dopamine'. *Electronic J. Biotechnol.*, 2014, **17**, pp. 183–188.
[7] Subramanian S.B., Francis A.P., Devasena T.: 'Chitosan–starch nanocomposite particles as a drug carrier for the delivery of bisdesmethoxy curcumin analog', *Carbohydr. Polym.*, 2014, **114**, pp. 170–178
[8] Vilar V.J., Botelho C.M., Boaventura R.A.: 'Methylene blue adsorption by algal biomass based materials: biosorbents characterization and process behaviour', *J. Hazard. Mater.*, 2007, **147**, pp. 120–132
[9] Acemioğlu B.: 'Adsorption of Congo red from aqueous solution onto calcium-rich fly ash', *J. Colloid Interface Sci.*, 2004, **274**, pp. 371–379
[10] Gupta V.K., Saleh T.A.: 'Sorption of pollutants by porous carbon, carbon nanotubes and fullerene- an overview', *Environ. Sci. Pollut. Res. Int.*, 2013, **20**, pp. 2828–2843
[11] Murty M., Chary N., Prabhakar S., *ET AL.*: 'Simultaneous quantitative determination of Sudan dyes using liquid chromatography–atmospheric pressure photoionization–tandem mass spectrometry'. *Food Chem.*, 2009, **115**, pp. 1556–1562.
[12] Yun M., Choe J.E., You J., *ET AL.*: 'High catalytic activity of electrochemically reduced graphene composite toward electrochemical sensing of Orange II'. *Food Chem.*, 2015, **169**, pp. 114–119.
[13] Saravanan R., Karthikeyan S., Gupta V.K., *ET AL.*: 'Enhanced photocatalytic activity of ZnO/CuO nanocomposite for the degradation of textile dye on visible light illumination', *Mater. Sci. Eng. C.*, 2013, **33**, pp. 91–98
[14] Saravanan R., Joicy S., Gupta V.K., Narayanan V., Stephen A.: 'Visible light induced degradation of methylene blue using CeO2/V2O5 and CeO2/CuO catalysts. *Mater. Sci. Eng., C.*, 2013, **33**, pp. 4725–4731.
[15] Saravanan R., Gracia F., Khan M.M., *ET AL.*: 'ZnO/CdO nanocomposites for textile effluent degradation and electrochemical detection', *J. Mol. Liq.*, 2015, **209**, pp. 374–380
[16] Shemshadi R.: 'Application of synthetic polymers as adsorbents for the removal of cadmium from aqueous solutions: batch experimental studies', *Caspian J. Environ. Sci.*, 2012, **10**, pp. 1–8
[17] Mittal A., Kaur D., Malviya A., *ET AL.*: 'Adsorption studies on the removal of coloring agent phenol red from wastewater using waste materials as adsorbents', *J. Colloid Interface Sci.*, 2009, **337**, pp. 345–354
[18] Mittal A., Mittal J., Malviya A., *ET AL.*: 'Removal and recovery of Chrysoidine Y from aqueous solutions by waste materials', *J. Colloid Interface Sci.*, 2010, **344**, pp. 497–507
[19] Zhu H.-Y., Jiang R., Xiao L.: 'Adsorption of an anionic azo dye by chitosan/kaolin/γ-$Fe_2O_3$ composites', *Appl. Clay Sci.*, 2010, **48**, pp. 522–526
[20] Zhu H., Jiang R., Fu Y., *ET AL.*: 'Preparation, characterization and dye adsorption properties of γ-Fe2O3/SiO2/chitosan composite'. *App. Surf. Sci.*, 2011, **258**, pp. 1337–1344.
[21] Tan I., Ahmad A., Hameed B.: 'Adsorption of basic dye using activated carbon prepared from oil palm shell: batch and fixed bed studies', *Desalination*, 2008, **225**, pp. 13–28
[22] Demirbas A.: 'Agricultural based activated carbons for the removal of dyes from aqueous solutions: a review', *J. Hazard. Mater.*, 2009, **167**, pp. 1–9
[23] Gupta V.: 'Application of low-cost adsorbents for dye removal–a review', *J. Environ. Manage.*, 2009, **90**, pp. 2313–2342
[24] Liu Y., Zheng Y., Wang A.: 'Enhanced adsorption of methylene blue from aqueous solution by chitosan-g-poly (acrylic acid)/vermiculite hydrogel composites', *J. Environ. Sci.*, 2010, **22**, pp. 486–493
[25] Rafatullah M., Sulaiman O., Hashim R., *ET AL.*: 'Adsorption of methylene blue on low-cost adsorbents: a review'. *J. Hazard. Mater.*, 2010, **177**, pp. 70–80.
[26] Balarak D., Jaafari J., Hassani G., *ET AL.*: 'The use of low-cost adsorbent (Canola residues) for the adsorption of methylene blue from aqueous solution: isotherm, kinetic and thermodynamic studies', *J. Colloid Interface Sci. Commun.*, 2015, **7**, pp. 16–19
[27] Deng J.H., Zhang X.R., Zeng G.M., *ET AL.*: 'Simultaneous removal of Cd(II) and ionic dyes from aqueous solution using magnetic graphene oxide nanocomposite as an adsorbent', *Chem. Eng. J.*, 2013, **226**, pp. 189–200
[28] Bée A., Obeid A., Mbolantenaina R., *ET AL.*: 'Magnetic chitosan/clay beads: a magsorbent for the removal of cationic dye from water', *J. Magn. Magn. Mater.*, 2017, **421**, pp. 59–64
[29] Al-Degs Y., Khraisheh M.A.M., Allen S.J., *ET AL.*: 'Adsorption characteristics of reactive dyes in columns of activated carbon'. *J. Hazard. Mater.*, 2009, **165**, pp. 944–949.
[30] Marandi R.: 'Biosorption of hexavalent chromium from aqueous solution by dead fungal biomass of phanerochaete crysosporium: batch and fixed bed studies', *Can. J. Chem. Eng. Technol.*, 2011, **2**, pp. 8–22
[31] Unuabonah E.I., Olu-Owolabi B.I., Fasuyi E.I., *ET AL.*: Modeling of fixed-bed column studies for the adsorption of cadmium onto novel polymer–clay composite adsorbent'. *J. Hazard. Mater.*, 2010, **179**, pp. 415–423.
[32] Lv L., Xie Y., Liu G., *ET AL.*: 'Removal of perchlorate from aqueous solution br cross-linked Fe(III)-chitosan complex', *J. Environ. Sci.*, 2014, **26**, pp. 792–800
[33] Jia Y., Xiao B., Thomas K.: 'Adsorption of metal ions on nitrogen surface functional groups in activated carbons', *Langmuir*, 2002, **18**, pp. 470–478
[34] Vijayakumar G., Tamilarasan R., Dharmendirakumar M.: 'Adsorption, kinetic, equilibrium and thermodynamic studies on the removal of basic dye Rhodamine-B from aqueous solution by the use of natural adsorbent perlite', *J. Mater. Environ. Sci.*, 2012, **3**, pp. 157–170
[35] Huang G., Zhang H., Shi J.X., *ET AL.*: 'Adsorption of chromium (VI) from aqueous solutions using cross-linked magnetic chitosan beads'. *Ind. Eng. Chem. Res.*, 2009, **48**, pp. 2646–2651.
[36] Yuwei C., Jianlong W.: 'Preparation and characterization of magnetic chitosan nanoparticles and its application for Cu (II) removal', *Chem. Eng. J.*, 2011, **168**, pp. 286–292
[37] Sadhasivam S., Savitha S., Swaminathan K.: 'Exploitation of Trichoderma harzianum mycelial waste for the removal of rhodamine 6G from aqueous solution', *J. Environ. Manage.*, 2007, **85**, pp. 155–161
[38] Jamal R., Zhang L., Wang M., *ET AL.*: 'Synthesis of poly (3,4-propylenedioxythiophene)/$MnO_2$ composites and their applications in the adsorptive removal of methylene blue', *Prog. Nat. Sci.*, 2016, **26**, pp. 32–40
[39] Zhang J., Zhou Y., Jiang M., *ET AL.*: 'Removal of methylene blue from aqueous solution by adsorption on pyrophyllite', *J. Mol. Liq.*, 2015, **209**, pp. 267–271
[40] Hammed A.K., Dewayanto N., Du D., *ET AL.*: 'Novel modified ZSM-5 as an efficient adsorbent for methylene blue removal', *J. Environ. Chem. Eng.*, 2016, **4**, pp. 2607–2616
[41] Zamani A., Shokri R., Yaftian M.R., *ET AL.*: 'Adsorption of lead, zinc and cadmium ions from contaminated water onto Peganum harmala seeds as biosorbent'. *Int. J. Environ. Sci. Technol.*, 2013, **10**, pp. 93–102.
[42] Gupta V.K., Mittal A., Jhare D., *ET AL.*: 'Batch and bulk removal of hazardous colouring Rose Bengal by adsorption techniques using bottom ash as adsorbent', *RSC Adv.*, 2012, **2**, pp. 8359–8381